Immunophenotyping of Stage III Melanoma Reveals Parameters Associated with Patient Prognosis

Nicolas Jacquelot, Maria Paula Roberti, David P. Enot, Sylvie Rusakiewicz, Michaela Semeraro, Sarah Jégou, Camila Flores, Lieping Chen, Byoung S. Kwon, Christophe Borg, et al.

Immunophenotyping of Stage III Melanoma Reveals Parameters Associated with Patient Prognosis

Nicolas Jacquelot[1,2,3,25], María Paula Roberti[1,3,4,25], David P. Enot[3,5,25], Sylvie Rusakiewicz[1,3,4], Michaela Semeraro[1,3,6], Sarah Jégou[7], Camila Flores[3], Lieping Chen[8], Byoung S. Kwon[9,10], Christophe Borg[11,12,13], Benjamin Weide[14], François Aubin[15], Stéphane Dalle[16], Holbrook Kohrt[17], Maha Ayyoub[1,2,3,4], Guido Kroemer[3,5,18,19,20,21,22], Aurélien Marabelle[1,3,4], Andréa Cavalcanti[3,23,24], Alexander Eggermont[3,25] and Laurence Zitvogel[1,2,3,4,25]

Stage III metastatic melanomas require adequate adjuvant immunotherapy to prevent relapses. Prognostic factors are awaited to optimize the clinical management of these patients. The magnitude of metastatic lymph node invasion and the *BRAF*^{V600} activating mutation have clinical significance. Based on a comprehensive immunophenotyping of 252 parameters per patient in paired blood and metastatic lymph nodes performed in 39 metastatic melanomas, we found that blood markers were as contributive as tumor-infiltrated lymphocyte immunotypes, and parameters associated with lymphocyte exhaustion/suppression showed higher clinical significance than those related to activation or lineage. High frequencies of CD45RA^{+}CD4^{+} and CD3^{-}CD56^{-} tumor-infiltrated lymphocytes appear to be independent prognostic factors of short progression-free survival. High NKG2D expression on CD8^{+}tumor-infiltrated lymphocytes, low level of regulatory T-cell tumor-infiltrated lymphocytes, and low PD-L1 expression on circulating T cells were retained in the multivariate Cox analysis model to predict prolonged overall survival. Prospective studies are needed to determine whether such immunological markers may guide adjuvant therapies in stage III metastatic melanomas.

Journal of Investigative Dermatology (2016) **136,** 994–1001; doi:10.1016/j.jid.2015.12.042

INTRODUCTION

Cutaneous melanoma is the major cause of mortality among skin malignancies (Eggermont et al., 2014). The prognostic factors for primary melanomas are Breslow thickness, ulceration, and mitotic index (Balch et al., 2009; Thompson et al., 2011). In stage III melanoma, the major prognostic factors are microscopic versus palpable nodal disease, number of positive nodes, and ulceration of the primary lesion (Balch et al., 2010). In stage IV melanoma, skin/subcutaneous tissue metastases and low serum levels of lactate dehydrogenase are associated with a better prognosis than are lung or other distant metastases and high lactate dehydrogenase (Balch et al., 2009). In the pioneering study of Erdag et al. (2012), higher counts of CD45^{+}, CD138^{+}, CD20^{+}, CD3^{+}, CD8^{+}, and PD-1^{+} tumor-infiltrated lymphocytes (TILs; assessed by comprehensive immunohistochemistry analyses of stage IV metastatic melanoma [MM] lesions) were all independently associated with better survival after adjusting for key clinical covariates, whereas abundances of CD4^{+} T cells, regulatory T cells (Tregs), natural killer (NK) lymphocytes, mature dendritic cells, or macrophages were not (Erdag et al., 2012).

[1]*INSERM U1015, Gustave Roussy Cancer Center, Villejuif, France;* [2]*University Paris Saclay, Kremlin Bicêtre, France;* [3]*Gustave Roussy Cancer Center, Villejuif, France;* [4]*CIC Biothérapie IGR Curie CIC1428, Gustave Roussy Cancer Center, Villejuif, France;* [5]*Metabolomics and Cell Biology Platforms, Gustave Roussy Cancer Center, Villejuif, France;* [6]*Center of Clinical Investigation, Hôpital Necker Enfants Malades, Paris, France;* [7]*Saint Antoine Hospital, INSERM ERL 1157-CNRS UMR 7203, Paris, France;* [8]*Department of Immunobiology, Yale School of Medicine, New Haven, Connecticut, USA;* [9]*Cancer Immunology Branch, Division of Cancer Biology, National Cancer Center, Ilsan, Goyang, Gyeonggi, Korea;* [10]*Section of Clinical Immunology, Allergy, and Rheumatology, Department of Medicine, Tulane University Health Sciences Center, New Orleans, Louisiana, USA;* [11]*Department of Medical Oncology, University Hospital of Besancon, Besancon, France;* [12]*Clinical Investigational Centre, CIC-1431, University Hospital of Besançon, Besançon, France;* [13]*INSERM U1098, University of Franche-Comté, Besançon, France;* [14]*Division of Dermatooncology, Department of Dermatology, University Medical Center Tübingen, Tübingen, Germany;* [15]*Université de Franche Comté, Service de Dermatologie, Centre Hospitalier Universitaire (CHU), Besançon, France;* [16]*Centre Hospitalier Lyon-Sud, Hospices Civils de Lyon and University Claude Bernard Lyon 1, Lyon, France;* [17]*Division of Oncology, Department of Medicine, Stanford University, Stanford, California, USA;* [18]*INSERM U1138, Centre de Recherche des Cordeliers, Paris, France;* [19]*Equipe 11 labellisée par la Ligue contre le Cancer, Centre de Recherche des Cordeliers, Paris, France;* [20]*Université Paris Descartes, Sorbonne Paris Cité, Paris, France;* [21]*Université Pierre et Marie Curie, Paris, France;* [22]*Pôle de Biologie, Hôpital Européen Georges Pompidou, AP-HP, Paris, France;* [23]*Department of Surgery, Gustave Roussy Cancer Center, Villejuif, France;* and [24]*Department of Dermatology, Gustave Roussy Cancer Center, Villejuif, France*

[25] *These authors contributed equally to this work.*

Correspondence: Laurence Zitvogel, Gustave Roussy Cancer Center, 114 rue Edouard Vaillant, 94805 Villejuif Cedex, France. E-mail: laurence.zitvogel@gustaveroussy.fr

Abbreviations: CTL, cytotoxic T lymphocyte; LN, lymph node; mLN, metastatic lymph node; MM, metastatic melanoma; NK, natural killer; OS, overall survival; PFS, progression-free survival; TIL, tumor-infiltrated lymphocyte

Received 24 September 2015; revised 8 December 2015; accepted 18 December 2015; accepted manuscript published online 29 January 2016; corrected proof published online 5 March 2016

The understanding of genetic heterogeneity of MM has revolutionized its clinical management. The discovery that 40–45% of melanomas harbor *BRAF* activating mutations, mostly at codon V600, launched a burst of targeted therapies involving BRAF and then MEK inhibitors (Chapman et al., 2011; Hauschild et al., 2012). Apart from cell autonomous effects associated with blocking oncogene addiction, BRAF inhibitors mediate their bioactivity on tumor-host interaction by inhibiting suppressive cytokines (such as IL-10, IL-6, vascular endothelial growth factor) (Sumimoto et al., 2006), reinstating dendritic cell function (Ott et al., 2013), increasing melanoma antigen presentation (Frederick et al., 2013), and T-cell activation (Boni et al., 2010; Frederick et al., 2013), leading to increased clonality of TILs (Cooper et al., 2013). However, distinct hallmarks of resistance to adaptive immunity occur after BRAF inhibition, such as MEK- and PI3K-dependent PD-L1 expression on tumor cells (Frederick et al., 2013; Jiang et al., 2013). PD-L1 up-regulation has been associated with high TIL content and IFN-γ–producing TILs (Kluger et al., 2015; Taube et al., 2012), but contradictory results about PD-L1 expression and prognosis of MM have been reported (Kluger et al., 2015; Massi et al., 2015). Indeed, $CD8^+$ T cells recognizing melanoma antigens eventually express exhaustion markers such as PD-1, the receptor for PD-L1, and/or CTLA-4, Tim-3, Lag3, KIR, and other immune checkpoints, thereby exhibiting impaired IFN-γ and IL-2 secretion (Ahmadzadeh et al., 2009; Baitsch et al., 2011). Hence, immunotherapy of MM has come of age with the recent success of immune checkpoint blockers (Eggermont et al., 2015). A number of studies have shown the prognostic impact of cytotoxic or Tregs circulating in the blood or residing in primary or metastatic lesions (Oble et al., 2009). A few studies performed in sentinel lymph nodes using immunohistochemistry, gene profiling, or flow cytometry described several mechanisms of immune subversion on melanoma antigen-specific T cells (Straten et al., 2006), such as Tregs (Mohos et al., 2013), distinct dendritic cell subtypes (Elliott et al., 2007), and specific receptors (Vallacchi et al., 2014). Because these results were controversial (Camisaschi et al., 2014), we undertook a comprehensive immunophenotyping of paired blood and metastatic lymph nodes (mLN) including 252 immune parameters (lineage-, activation-, exhaustion-related markers) to harness the most robust immune profiles endowed with clinical significance for progression-free survival (PFS) or overall survival (OS). Here we describe immunotypes corresponding to specific clinical traits as well as blood or tumor parameters associated with PFS and OS. These immunophenotypes should be validated prospectively and may guide future studies using immune checkpoint blockers or immunomodulators.

RESULTS AND DISCUSSION

Immunotypes associated with lymph node invasion and *BRAF*^{V600} mutation

The patient cohort consisting of 39 MMs that benefited from surgery for mLN is described in Supplementary Table S1 (online), with their survival curves shown in Supplementary Figure S1 (online). Immediately after mechanical and enzymatic digestion of mLN, tumor and blood compositions were analyzed in a paired manner for 25 patients by flow cytometry (antibodies listed in Supplementary Table S2 online), with the gating strategy exemplified in Supplementary Figure S2 (online). Of the 337 parameters initially selected, 252 were found to be robustly quantified, with 124 and 128 in blood and tumor, respectively. They reflect multiple cellular types, activation status, naïve or memory phenotypes, and activating or inhibitory receptors and ligands. The markers are shown in the form of dependency networks in Supplementary Figures S3 and S4 (online), which illustrate the complexity of the immune tone. However, no reliable clustering of markers could be found.

Briefly, mLN contained about 27% $CD45^+$ live cells (see Supplementary Figure S5a online), enriched in $CD3^+$ T cells compared to blood (see Supplementary Figure S5b), more specifically $CD4^+$ T cells (see Supplementary Figure S5c). NK cells were underrepresented in tumor beds (see Supplementary Figure S5d), as previously observed (Messaoudene et al., 2014). About 41% of $CD4^+$ TILs and 54% of $CD8^+$ TILs (cytotoxic T lymphocytes [CTLs]) produced IFN-γ (>2%) and proliferated ($Ki67^+$ cells), whereas about 90% of TILs secreted tumor necrosis factor-α (>2%) after ex vivo stimulation (see Supplementary Figure S5e). Most of these CTLs were highly activated as assessed by CD69 (see Supplementary Figure S6a online), as described for hepatocellular carcinoma (Chen et al., 2007) and CD27, CD137, CD95, and CD137L expression levels (see Supplementary Figure S6b–e). Expression of inhibitory receptors (such as PD-1, Tim-3) and their ligand PD-L1 on T and NK cells is shown in Supplementary Figure S6f–i. In accordance with previous reports (Tumeh et al., 2014), PD-L1 expression on intratumoral as well as blood T cells was not insignificant.

We next investigated immunological traits associated with classic prognostic parameters of melanoma. Significant markers are all summarized in Supplementary Tables S3 and S4 (online) (blood- and tumor-related markers, respectively, arbitrarily setting the threshold of significance at a raw *P*-value of 0.05).

The number of invaded LN (>3N+) was associated with a dismal prognosis in these stage III MMs (see Supplementary Figure S7a online). We observed a drop in circulating $CD4^+$ T cells (Figure 1a), whereas $CD4^+$ T cells increased in tumor (compared with poorly disseminated diseases; see Supplementary Figure S7b). Highly invaded LN contained few $PD\text{-}1^+CD8^+$ T cells (Figure 1b), a trait associated with a lower $PD\text{-}1^+Tim\text{-}3^+CD8^+$/Treg ratio (see Supplementary Figure S7c), and the $CD8^+$/Treg ratio was correlated with CTLs (see Supplementary Figure S7d). Additionally, $CD3^-CD56^-$ cells comprising B cells and major histocompatibility complex class II^{low} myeloid cells of granulocytic origin (see Supplementary Figure S8 online) lost CD137L expression cells in both compartments in heavily invaded LN (Figure 1c and Supplementary Figure S7e). In accordance with our data, CD137L-expressing B cells are known to represent an evolutionary conserved subset of memory B cells with antimetastatic properties that accumulates in the elderly and correlates with granzyme B^+ $CD8^+$ T cells (Lee-Chang et al., 2014). Moreover, activation markers on NK cells, already reported as being associated with functional activity and prognosis (Ali et al., 2014), decreased with

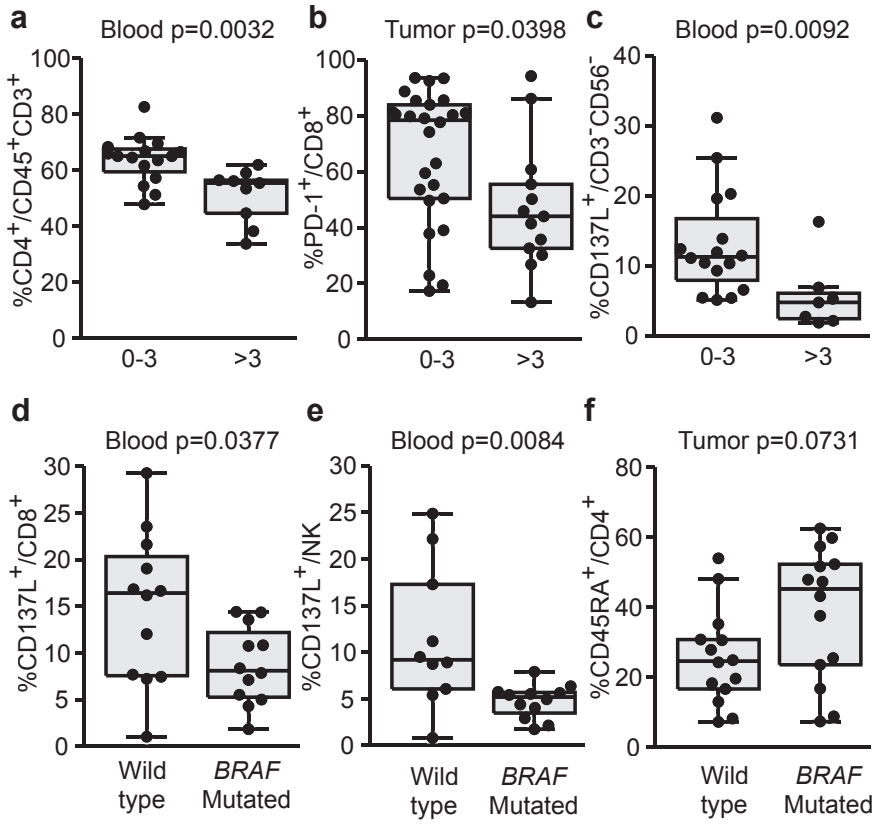

Figure 1. Immunotypes associated with the *BRAF*^{V600} mutation and the severity of lymph node invasion. Drop in (**a**) circulating CD4$^+$ and (**b**) intratumoral CD8$^+$PD-1$^+$ T-cell proportions according to metastatic lymph node invasion. (**c**) Distribution in blood of CD137L$^+$CD3$^-$CD56$^-$ cells according to the number of invaded lymph nodes. Decreased CD137L expression in distinct circulating leukocyte subset in patients harboring *BRAF*^{V600} mutated tumors. (**d, e**) Flow cytometric analyses of blood leukocytes assessing CD137L expression on (**d**) CD8$^+$ or (**e**) NK cells. (**f**) Increased percentages of CD45RA$^+$CD4$^+$ T cells in tumor-infiltrated lymphocytes from mutated tumors as assessed by flow cytometry. Each dot represents one patient. Wilcoxon Rank-Sum test: all *P*-values are indicated.

mLN invasion, in particular PD-L1 and CD137L (see Supplementary Figure S7f). All of these data suggest that once tumor cells operate an exodus from lymph nodes, dissemination of the disease might induce a coordinated dysfunction of several components of the immune system concomitantly.

The *BRAF*^{V600} oncogenic mutation was an independent prognosis factor associated with shorter OS (see Supplementary Figure S9a online). The immunological hallmarks associated with the activating *BRAF*^{V600} mutation were a drop in blood CD137L- and PD-L1–expressing CD8$^+$ T cells (Figure 1d and Supplementary Figure S9b) and a profound decrease in CD137L$^+$ circulating NK cells (Figure 1e). In addition, the CD4$^+$ T-cell compartment in tumor beds was altered with a trend toward an increase of naïve CD45RA$^+$CD4$^+$ T cells (Figure 1f) and a drop in Lag3-expressing Tregs (see Supplementary Figure S9c).

Stage III MMs contain CD45RA$^+$CD4$^+$ TILs and Treg inversely correlating with intratumoral CTLs and OS

At the expense of CD4$^+$ T cells, intratumoral accumulation of CTLs in mLN are known to be of favorable prognosis in MM (Bogunovic et al., 2009; Mihm et al., 1996; Oble et al., 2009). Among CD4$^+$ TILs, a large proportions were CD45RA$^+$CD4$^+$ T cells, with about 83% of naïve CD45RA$^+$CCR7$^+$cells (not shown) that anticorrelated with CTLs and PD1$^+$CD8$^+$ TILs (Figure 2a–c). When classifying our 252 immunological markers determined in blood and tumor beds according to their clinical significance in stage III–IV MM, we concluded that high proportions of naive CD45RA$^+$CD4$^+$ TILs were associated with rapid disease progression (Figure 2d) and remained significant after adjusting for mLN invasion, therefore adding prognostic value to local aggressiveness (hazard ratio = 4.3 and 3.1, respectively).

Besides naïve T cells, the CD4$^+$ TIL fraction contained a high proportion of CD25^{high}CD127$^-$CD4$^+$ Tregs (Figure 3a), which correlated with the activation status of CD4$^+$ and CD8$^+$ T cells (CD69 and PD-1/TIM3 expression, respectively; Figure 3b and c). When stratifying on the *BRAF* mutational status, we observed that the proportions of Treg TILs dictated OS, with the worse subgroup of patients being those harboring a *BRAF*^{V600} MM and high percentages of Treg (above the median; Figure 3d).

Tumoral NKG2D and blood PDL-1 expression on CD8$^+$ T cells influence OS in stage III MM

NKG2D is an important activating receptor associated with cytolytic functions of CTL and NK cells (Diefenbach et al., 2001). NKG2D engagement is dictated by the presence of their major histocompatibility complex class I- like ligands expressed by tumor cells (mainly MICA/B and ULBP2 in melanoma) (Paschen et al., 2009). Tumor-associated metalloproteinases induce ligand release, NKG2D engagement, and functional defects (Paschen et al., 2009; Waldhauer and Steinle, 2006). In contrast to stage IV MM (Romero et al., 2014), stage III melanoma maintained high expressions of NKG2D receptors in blood (Figure 4a and data not shown), but such expressions decreased in tumor beds in many patients, a trait relevant for OS (hazard ratio = 0.15 after adjusting for most significant covariates). When combined with *BRAF* mutation, very high percentages of

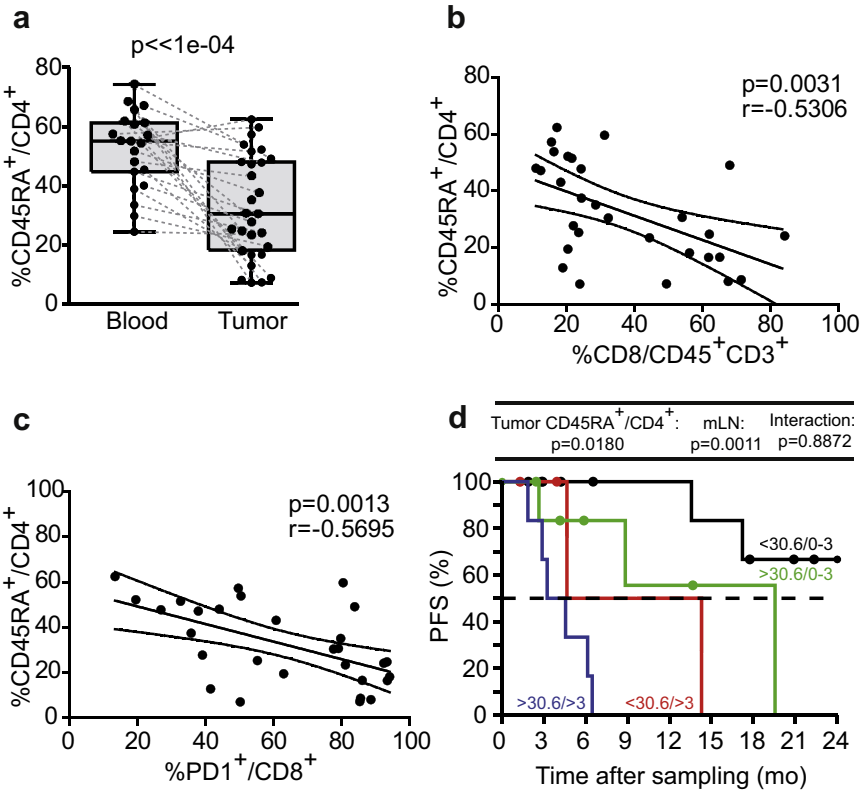

Figure 2. Naïve CD45RA$^+$CD4$^+$ T cells inversely correlated with intratumoral cytotoxic T lymphocytes and were associated with shorter progression-free survival (PFS). (**a**) Flow cytometric analyses of blood leukocytes and tumor-infiltrated lymphocytes (TILs) assessing the lineage-related marker CD45RA in CD4$^+$ T cells in a paired manner. (**b, c**) Spearman correlations between the percentages of CD4$^+$CD45RA$^+$ TILs and CD8$^+$ cytotoxic T lymphocytes or PD1$^+$CD8$^+$ TILs. Each dot represents one patient. Wilcoxon paired signed-rank and Spearman correlation tests: *P*-values are indicated. (**d**) Kaplan-Meier PFS curves segregating the cohort of metastatic melanoma patients according to the median value of CD4$^+$CD45RA$^+$ TILs retained in the Cox multivariate model in tumor analyses. Likelihood ratio tests from Cox regression modeling are used to assess the prognostic value for the marker with and without accounting for metastatic lymph node (mLN) invasion status (0–3 vs >3).

NKG2D$^+$CD8$^+$ TILs protected against the *BRAF* mutation-associated dismal prognosis (Figure 4b). With the exception of two, all patients presenting a *BRAF* mutation but high NKG2D expression on CD8$^+$ TILs survived >2 years.

The expression of inhibitory receptors (PD-1, TIM3, CTLA-4) was higher in TILs than blood cells and more in CD8$^+$ than CD4$^+$ TILs, except for CTLA-4 expression (see Supplementary Figure S6f and g and data not shown). In contrast, PD-L1, the ligand for PD-1, was equally expressed in almost all leukocyte subsets in blood and tumor beds (see Supplementary Figure S6h and Figure 4c, upper panel). Interestingly, the mean fluorescence intensity of PD-L1 expression (compared with that of the isotype control antibody) on the surface of circulating CD8$^+$ T cells (or CD4$^+$ T cells; see Supplementary Figure S10a online) correlated with the percentages of PD-L1$^+$CD8$^+$ T cells (Figure 4c, lower panel) and PD-L1$^+$CD4$^+$ T cells (see Supplementary Figure S10b). In accordance with Chevolet et al. (2015), high expression levels of PD-L1 on CD4$^+$ and CD8$^+$ T lymphocytes were associated with a bad prognosis, even more so in the presence of the *BRAF* paradigmatic mutation (Figure 4d and Supplementary Figure S10c). PD-L1 is expressed on a subset of melanoma, most likely as a consequence of lymphocytic infiltrates, in particular IFN-γ–producing CTLs (Massi et al., 2015; Taube et al., 2012). However, PD-L1 can also be expressed by immune cells at similar levels as in tumor cells and equally well in blood and tumor compartments, in a coordinated manner in all cell types (CD4$^+$ T, CD8$^+$ T, NK, CD45$^-$, CD3$^-$CD56$^-$; see Supplementary Figures S3, S4, and S6). Chevolet et al. (2015) reported an interconnected overexpression of IDO, PD-L1, and CTLA-4 in peripheral blood leukocytes in MM, associated with advanced disease and negative clinical outcome. High levels of circulating PD-L1–expressing CTLs and CTLA-4–expressing Treg conferred a negative prognosis.

Dismal prognosis role for non-T cells and non-NK cells in the tumor of stage III MM

CD3$^-$CD56$^-$ cells, comprising B cells and major histocompatibility complex class II^{low} myeloid cells of granulocytic origin (see Supplementary Figure S8), were not increased in the tumor microenvironment (Figure 5a). However, their blood phenotype was modified by the presence of tumor cells at a distant site in that they lost their CD137L expression in cases of heavily invaded stage III MM (Figure 1c). Supporting their regulatory role, their proportions are negatively and positively correlated with the favorable CTL TILs and the bad prognosis CD4$^+$CD45RA$^+$ TIL subset, respectively (Figure 5b and c). High intratumoral CD3$^-$CD56$^-$ cells were associated with short PFS, even in cases of poorly invaded LN (Figure 5d).

Overall, when classifying our 252 immunological markers determined in blood and tumor beds according to their biological (lineage vs. activation vs. exhaustion; see Supplementary Tables S3 and S4) and clinical significance (>3N+, capsular rupture, *BRAF* mutational status, ulceration status, and gender; see Supplementary Figure S11 online) in stage III–IV MM, we concluded that (i) both blood and tumor markers equally contributed to defining the prognosis, (ii) exhaustion markers markedly affected the clinical outcome, and (iii) activation markers appeared less relevant for the functional study of tumor beds (see Supplementary

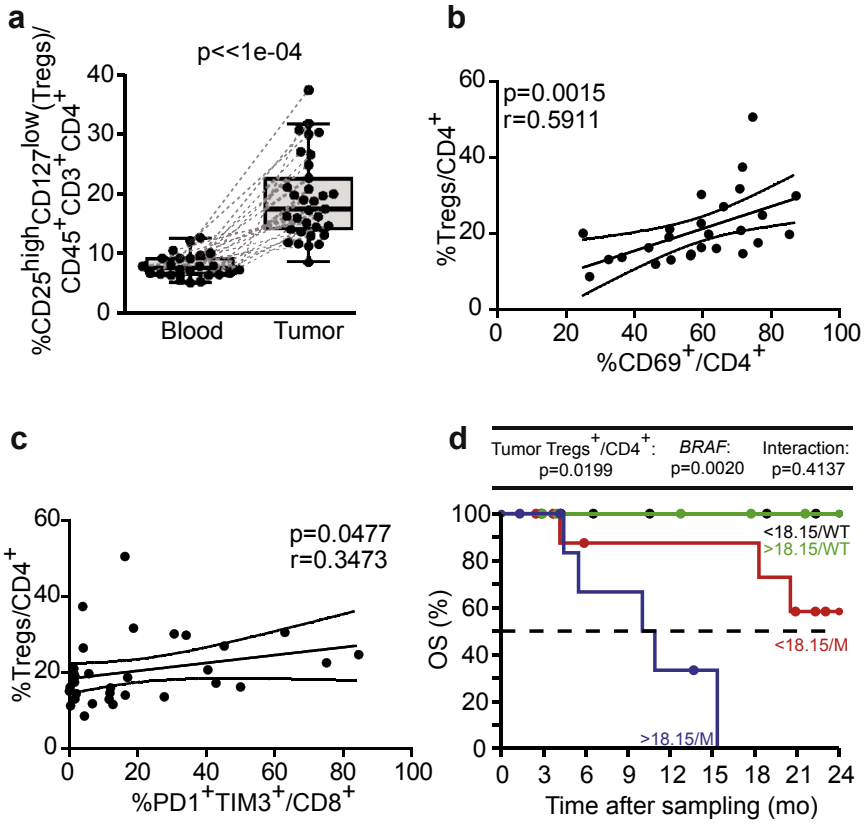

Figure 3. Regulatory T-cell (Treg) tumor-infiltrating lymphocytes (TILs) negatively impact on overall survival (OS) and overrule *BRAF* mutational status. (**a**) Flow cytometric analyses of blood leukocytes and tumor infiltrating cells assessing the $CD127^{-}CD25^{high}$ cells in $CD4^{+}$ TILs (Treg) in a paired manner. (**b, c**) Spearman correlations between the percentages of Treg and (**b**) $CD4^{+}CD69^{+}$ TILs and (**c**) $CD8^{+}PD1^{+}TIM3^{+}$ TILs. Each dot represents one patient. Wilcoxon paired signed-rank and Spearman correlation tests: *P*-values are indicated. (**d**) Kaplan-Meier OS curves segregating the cohort of metastatic melanoma patients according to the median value of Treg TILs retained in the Cox multivariate model in tumor analyses. Likelihood ratio tests from Cox regression modeling are used to assess the prognostic value for the marker with and without accounting for *BRAF* mutational status (mutated [M] vs wild type [WT]).

Figure S12 online). In our panels, we found (arbitrarily setting the threshold of significance at a raw *P*-value of 0.05), that only a few markers (just six) may represent prognostic factors influencing PFS or OS in blood or tumor beds independently of clinicopathological parameters in multivariate Cox regression analyses. Of note, specimen sampling after neoadjuvant therapy did not influence these results. Altogether, all the modulations of the components of natural immunosurveillance against stage III MM described in this study deserve to be validated prospectively in order to be followed in the course of the development of monoclonal antibody therapies.

MATERIALS AND METHODS

Patient characteristics

For the Gustave Roussy Cancer Campus cohort, patients >18 years old with histologically confirmed metastatic and/or resectable melanoma provided written informed consent according to protocols reviewed and approved by the institutional ethic committee, including the investigator-sponsored MSN study (NCT02105168). For the Centre Hospitalier Lyon Sud cohort, patients >18 years old with histologically confirmed metastatic and/or resectable (for all stage III) melanoma were included in the study. All patients provided informed consent before enrollment. Patient characteristics are described in Supplementary Table S1.

Peripheral blood mononuclear cell preparations

Peripheral blood samples from patients drawn just before surgery were carefully layered on top of a Ficoll-Hypaque density gradient media (PAA Laboratories, Coelbe, Germany). For all relevant parameters described in this study, the neoadjuvant treatment administered before blood and tumor sampling did not significantly impact on the results (see Supplementary Table S1 and data not shown).

TIL preparations

Resected mLN specimens from MM patients were placed in isotonic solution at least for 1 hour. These media (secretome) were frozen until protein dosage. Next, tissue was cut and placed in dissociation medium, which consisted of RPMI1640, 1% penicillin/streptomycin (PEST, Gibco Invitrogen, Grand Island, NY), collagenase IV (50 IU/ml), hyaluronidase (280 IU/ml), and DNAse I (30 IU/ml) (all from Sigma-Aldrich, St. Louis, MO), and run on a gentleMACS dissociator (Miltenyi Biotec, Bergisch Gladbach, Germany). Dissociation time lasted 1 hour under mechanical rotation and did not influence the results of the phenotyping. Cell samples were diluted in phosphate buffered saline, passed through a cell strainer, and centrifuged for 5 minutes at 1,500 r.p.m. Cells were finally resuspended in phosphate buffered saline, counted, stained for flow cytometric analyses, or resuspended in CryoMaxx medium (PAA Laboratories) for storage in liquid nitrogen. All mLNs included in the study were histologically confirmed to be invaded.

Flow cytometric analyses

For membranous labeling, peripheral blood mononuclear cells and TILs were stained with fluorochrome-coupled monoclonal antibodies (detailed in Supplementary Table S2), incubated for 20 minutes at 4 °C, and washed. Some dissociated cells from mLNs were incubated in 48-multiwell dishes at 0.3×10^{6} leukocytes per milliliter. After 18–24 hours of cell recovery cultured in complete medium (RPMI1640 supplemented with 10% human AB serum, 1% penicillin/streptomycin [PEST, Gibco Invitrogen], 1% L-glutamine [Gibco Invitrogen], and 1% sodium pyruvate [Gibco Invitrogen]), some of these cells were stimulated with phorbol 12-myristate 13-acetate (5 ng/ml; Sigma), ionomycin (125 ng/ml; Sigma), and

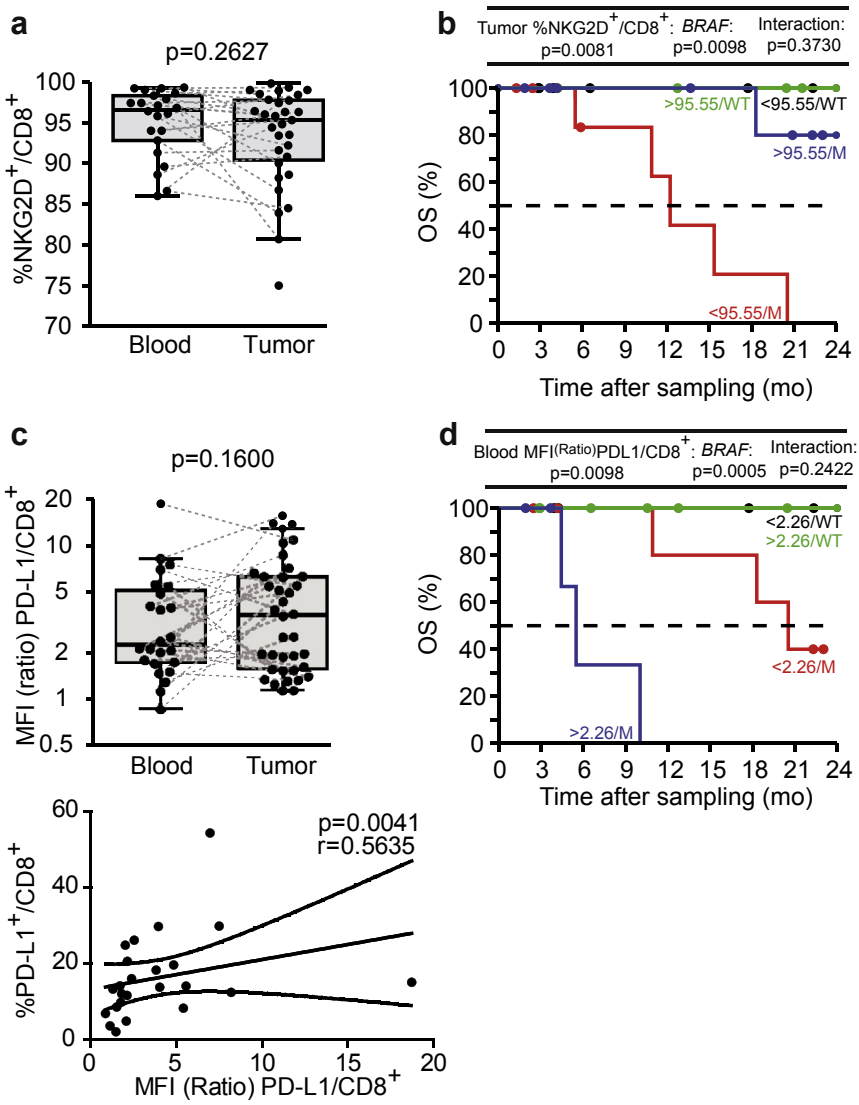

Figure 4. NKG2D and PDL-1 expression on CD8$^+$ tumor-infiltrated lymphocytes and blood cells influenced the prognosis of stage III metastatic melanoma. (**a**). Flow cytometric analyses of CD8$^+$ T cells for NKG2D expression and (**b**) prognosis value shown by Kaplan-Meier overall survival (OS) curves segregating the cohort of metastatic melanoma patients according to the median value of CD8$^+$NKG2D$^+$ tumor-infiltrated lymphocytes and *BRAF* mutational status (mutated [M] vs wild type [WT]) both retained in the Cox multivariate model. (**c**) Mean fluorescence intensity (MFI) of membrane expression of PD-L1 on CD8$^+$ blood T cells compared with the isotype control antibody MFI (ratio of MFI, upper panel) and its Spearman correlation with the percentages of circulating PD-L1$^+$CD8$^+$ T cells (lower panel). Wilcoxon paired signed-rank and Spearman correlation tests: *P*-values are indicated. (**d**) Same as **b** but using the MFI ratio of PD-L1 positivity on CD8$^+$ cytotoxic T lymphocytes for the Kaplan-Meier curve of OS.

BD Golgi Stop (4 µl/6 ml; BD Biosciences, San Jose, CA) during 3–5 hours and then harvested, membranous labeled to discriminate different lymphocyte subsets (see Supplementary Table S2), and permeabilized with BD Cytofix/Cytoperm kit (BD Biosciences). Intracellular staining was performed with anti–IFN-γ–PE (clone B27; BD Biosciences) and anti-tumor necrosis factor–α-AF647 (clone Mab11; BioLegend, San Diego, CA) antibodies following the manufacturer's protocol. For Ki67 staining, other cells was cultured for 4–5 days before assessment of proliferation status. Briefly, cells were harvested, membranous labeled, permeabilized with Foxp3/transcription factor fixation/permeabilization kit (eBiosciences, San Diego, CA), and intranuclear stained with anti–Ki67-PE (clone B56; BD Biosciences, San Diego, CA) antibody following the manufacturer's recommendations. Cell samples were acquired on a Cyan ADP 9-color flow cytometer (Beckman Coulter, Marseille, France) with single-stained antibody-capturing beads used for compensation (Compbeads, BD Biosciences). Data were analyzed with Flowjo software version 7.6.2 (Tree Star, Ashland, OR).

Cytokines and chemokines measurements

Tumor-conditioned supernatants were monitored using the human Th1/Th2/Th9/Th17/Th22 13-plex RTU FlowCytomix Kit (eBiosciences) and the human Chemokine 6 plex kit FlowCytomix (eBiosciences) according to the manufacturer's instructions and acquired on a Cyan ADP 9-color flow cytometer (Beckman Coulter). Analyses were performed by Flowcytomix Pro 3.0 Software (eBiosciences). CXCL10 (BD Biosciences) was measured by ELISA kit in accordance with the manufacturer's recommendations. All cytokines/chemokines were normalized to the total protein content as measured by the DC protein assay (Bio-Rad, Hercules, CA) following the manufacturer's protocol.

Statistical analysis

Data analyses and representations were performed with either Prism 5 (GraphPad, San Diego, CA) or within the statistical environment R (http://www.R-project.org/). In total, 124 (blood) and 128 (tumor) parameters were considered for analyses and reporting. Spearman test was applied to assess correlations between parameters (Prism 5). All remaining calculations were performed within R. Individual datapoints representing the measurement from one patient are systematically graphed alongside with the box and whisker plots calculated from the corresponding distribution. Comparisons between clinical groups were performed by beta regression for parameters expressed in percentage and by linear modeling for the other parameters and ratios

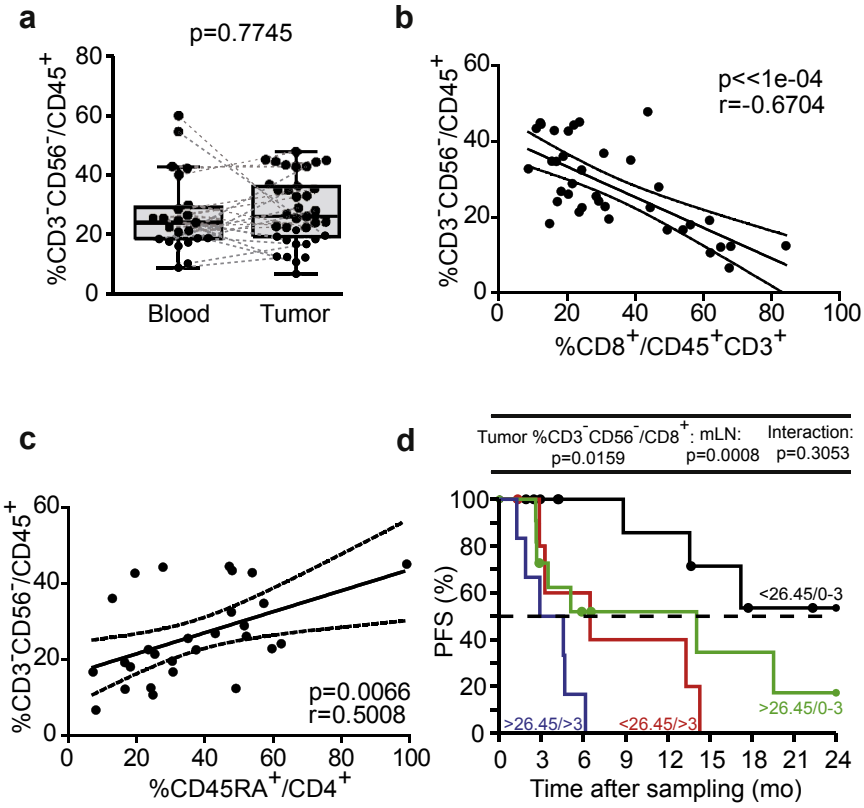

Figure 5. Tumor CD3$^-$CD56$^-$ cells inversely correlated with intratumoral cytotoxic T lymphocytes (CTLs) and negatively predicted progression-free survival (PFS). (**a**) Flow cytometric analyses of blood and tumor CD3$^-$CD56$^-$ cells performed in a paired manner. (**b, c**) Spearman correlations between CD3$^-$CD56$^-$ cells and (**b**) CD8$^+$ CTL tumor-infiltrated lymphocytes and (**c**) CD4$^+$CD45RA$^+$ tumor-infiltrated lymphocytes. Each dot represents one patient. Wilcoxon paired signed-rank and Spearman correlation tests: *P*-values are indicated. (**d**) Kaplan-Meier PFS curves segregating the cohort of metastatic melanoma patients according to the median value of tumor CD3$^-$CD56$^-$ cells retained in the Cox multivariate model in tumor analyses. Likelihood ratio tests from Cox regression modeling are used to assess the prognostic value for the marker with and without accounting for metastatic lymph node (mLN) invasion status (0–3 vs >3).

after log transformation. Dispersion was allowed to differ between groups, and contrasts of interest were back-transformed and presented as ratios. Wilcoxon signed-rank test was applied to assess differences in concentration between matching pairs of blood leukocytes and tumor-infiltrated cells samples. OS and progression-free survival (PFS) determined from the date of sampling were used as the primary endpoints. Survival curves were estimated by the Kaplan-Meier product-limit method. Survival distributions were compared by Firth penalized-likelihood Cox regression after stratifying for *BRAF* status, gender, number of mLNs, and disease stage. Flow cytometric parameters were converted to z-scores before computing the correlation matrices. Unless stated, *P*-values are two sided, and 95% confidence intervals for the statistic of interest are reported and were not adjusted for false discovery rate.

CONFLICT OF INTEREST

LC receives consulting fees from Medimmune and Pfizer and patent/licensing payments from Bristol-Myers Squibb. SD is principal investigator clinical trials with Bristol-Myers Squibb.

ACKNOWLEDGMENTS

The authors would like to thank the patients who participated in this study and our collaborators from the Surgery, Dermatology, and Biology and Pathology departments, and the Center of Biological Resources, for their essential contributions to this work. This work was supported by Ligue Contre le Cancer (Équipe Labellisée de LZ), ISREC Foundation, Fondation pour la Recherche Médicale (FRM), Institut National du Cancer (INCa), Cancéropôle Ile-de-France, the LabEx Immuno-Oncology, the SIRIC Stratified Oncology Cell DNA Repair and Tumor Immune Elimination (SOCRATE), the SIRIC Cancer Research and Personalized Medicine (CARPEM), the Paris Alliance of Cancer Research Institutes (PACRI). SIRIC SOCRATE (INCa/DGOS/INSERM 6043), LABEX OncoImmunology, Institut National du Cancer (INCa, 2012-062), Université Paris-Sud, and the PACRI network. This work was partially supported by NIH Grants CA142779, CA016359, and CA121974, and a United Technologies Corporation endowed chair to LC. NJ received a fellowship from Cancéropole Idf.

SUPPLEMENTARY MATERIAL

Supplementary material is linked to the online version of the paper at www.jidonline.org, and at http://dx.doi.org/10.1016/j.jid.2015.12.042.

REFERENCES

Ahmadzadeh M, Johnson LA, Heemskerk B, Wunderlich JR, Dudley ME, White DE, et al. Tumor antigen-specific CD8 T cells infiltrating the tumor express high levels of PD-1 and are functionally impaired. Blood 2009;114:1537–44.

Ali TH, Pisanti S, Ciaglia E, Mortarini R, Anichini A, Garofalo C, et al. Enrichment of CD56(dim)KIR + CD57 + highly cytotoxic NK cells in tumour-infiltrated lymph nodes of melanoma patients. Nat Commun 2014;5:5639.

Baitsch L, Baumgaertner P, Devêvre E, Raghav SK, Legat A, Barba L, et al. Exhaustion of tumor-specific CD8$^+$ T cells in metastases from melanoma patients. J Clin Invest 2011;121:2350–60.

Balch CM, Gershenwald JE, Soong S-J, Thompson JF, Atkins MB, Byrd DR, et al. Final version of 2009 AJCC melanoma staging and classification. J Clin Oncol Off J Am Soc Clin Oncol 2009;27:6199–206.

Balch CM, Gershenwald JE, Soong S-J, Thompson JF, Ding S, Byrd DR, et al. Multivariate analysis of prognostic factors among 2,313 patients with stage III melanoma: comparison of nodal micrometastases versus macrometastases. J Clin Oncol 2010;28:2452–9.

Bogunovic D, O'Neill DW, Belitskaya-Levy I, Vacic V, Yu Y-L, Adams S, et al. Immune profile and mitotic index of metastatic melanoma lesions enhance clinical staging in predicting patient survival. Proc Natl Acad Sci USA 2009;106:20429–34.

Boni A, Cogdill AP, Dang P, Udayakumar D, Njauw C-NJ, Sloss CM, et al. Selective BRAFV600E inhibition enhances T-cell recognition of melanoma without affecting lymphocyte function. Cancer Res 2010;70:5213–9.

Camisaschi C, Vallacchi V, Castelli C, Rivoltini L, Rodolfo M. Immune cells in the melanoma microenvironment hold information for prediction of the risk of recurrence and response to treatment. Expert Rev Mol Diagn 2014;14:643–6.

Chapman PB, Hauschild A, Robert C, Haanen JB, Ascierto P, Larkin J, et al. Improved survival with vemurafenib in melanoma with BRAF V600E mutation. N Engl J Med 2011;364:2507–16.

Chen C-H, Lee H-S, Huang G-T, Yang P-M, Yu W-Y, Cheng K-C, et al. Phenotypic analysis of tumor-infiltrating lymphocytes in hepatocellular carcinoma. Hepatogastroenterology 2007;54:1529–33.

Chevolet I, Speeckaert R, Schreuer M, Neyns B, Krysko O, Bachert C, et al. Characterization of the in vivo immune network of IDO, tryptophan metabolism, PD-L1, and CTLA-4 in circulating immune cells in melanoma. Oncoimmunology 2015;4:e982382.

Cooper ZA, Frederick DT, Juneja VR, Sullivan RJ, Lawrence DP, Piris A, et al. BRAF inhibition is associated with increased clonality in tumor-infiltrating lymphocytes. Oncoimmunology 2013;2:e26615.

Diefenbach A, Jensen ER, Jamieson AM, Raulet DH. Rae1 and H60 ligands of the NKG2D receptor stimulate tumour immunity. Nature 2001;413:165–71.

Eggermont AMM, Maio M, Robert C. Immune checkpoint inhibitors in melanoma provide the cornerstones for curative therapies. Semin Oncol 2015;42:429–35.

Eggermont AMM, Spatz A, Robert C. Cutaneous melanoma. Lancet 2014;383:816–27.

Elliott B, Scolyer RA, Suciu S, Lebecque S, Rimoldi D, Gugerli O, et al. Long-term protective effect of mature DC-LAMP+ dendritic cell accumulation in sentinel lymph nodes containing micrometastatic melanoma. Clin Cancer Res 2007;13:3825–30.

Erdag G, Schaefer JT, Smolkin ME, Deacon DH, Shea SM, Dengel LT, et al. Immunotype and immunohistologic characteristics of tumor-infiltrating immune cells are associated with clinical outcome in metastatic melanoma. Cancer Res 2012;72:1070–80.

Frederick DT, Piris A, Cogdill AP, Cooper ZA, Lezcano C, Ferrone CR, et al. BRAF inhibition is associated with enhanced melanoma antigen expression and a more favorable tumor microenvironment in patients with metastatic melanoma. Clin Cancer Res 2013;19:1225–31.

Hauschild A, Grob J-J, Demidov LV, Jouary T, Gutzmer R, Millward M, et al. Dabrafenib in BRAF-mutated metastatic melanoma: a multicentre, open-label, phase 3 randomised controlled trial. Lancet 2012;380:358–65.

Jiang X, Zhou J, Giobbie-Hurder A, Wargo J, Hodi FS. The activation of MAPK in melanoma cells resistant to BRAF inhibition promotes PD-L1 expression that is reversible by MEK and PI3K inhibition. Clin Cancer Res 2013;19:598–609.

Kluger HM, Zito CR, Barr ML, Baine MK, Chiang VLS, Sznol M, et al. Characterization of PD-L1 expression and associated T-cell infiltrates in metastatic melanoma samples from variable anatomic sites. Clin Cancer Res 2015;21:3052–60.

Lee-Chang C, Bodogai M, Moritoh K, Olkhanud PB, Chan AC, Croft M, et al. Accumulation of 4-1BBL+ B cells in the elderly induces the generation of granzyme-B+ CD8+ T cells with potential antitumor activity. Blood 2014;124:1450–9.

Massi D, Brusa D, Merelli B, Falcone C, Xue G, Carobbio A, et al. The status of PD-L1 and tumor-infiltrating immune cells predict resistance and poor prognosis in BRAFi-treated melanoma patients harboring mutant BRAFV600. Ann Oncol 2015;26:1980–7.

Messaoudene M, Fregni G, Fourmentraux-Neves E, Chanal J, Maubec E, Mazouz-Dorval S, et al. Mature cytotoxic CD56(bright)/CD16(+) natural killer cells can infiltrate lymph nodes adjacent to metastatic melanoma. Cancer Res 2014;74:81–92.

Mihm MC, Clemente CG, Cascinelli N. Tumor infiltrating lymphocytes in lymph node melanoma metastases: a histopathologic prognostic indicator and an expression of local immune response. Lab Invest 1996;74:43–7.

Mohos A, Sebestyén T, Liszkay G, Plótár V, Horváth S, Gaudi I, et al. Immune cell profile of sentinel lymph nodes in patients with malignant melanoma: FOXP3+ cell density in cases with positive sentinel node status is associated with unfavorable clinical outcome. J Transl Med 2013;11:43.

Oble DA, Loewe R, Yu P, Mihm MC. Focus on TILs: prognostic significance of tumor infiltrating lymphocytes in human melanoma. Cancer Immun 2009;9:3.

Ott PA, Henry T, Baranda SJ, Frleta D, Manches O, Bogunovic D, et al. Inhibition of both BRAF and MEK in BRAF(V600E) mutant melanoma restores compromised dendritic cell (DC) function while having differential direct effects on DC properties. Cancer Immunol Immunother 2013;62:811–22.

Paschen A, Sucker A, Hill B, Moll I, Zapatka M, Nguyen XD, et al. Differential clinical significance of individual NKG2D ligands in melanoma: soluble ULBP2 as an indicator of poor prognosis superior to S100B. Clin Cancer Res 2009;15:5208–15.

Romero AI, Chaput N, Poirier-Colame V, Rusakiewicz S, Jacquelot N, Chaba K, et al. Regulation of CD4(+)NKG2D(+) Th1 cells in patients with metastatic melanoma treated with sorafenib: role of IL-15Rα and NKG2D triggering. Cancer Res 2014;74:68–80.

Straten P thor, Dahl C, Schrama D, Pedersen LØ, Andersen MH, Seremet T, et al. Identification of identical TCRs in primary melanoma lesions and tumor free corresponding sentinel lymph nodes. Cancer Immunol Immunother 2006;55:495–502.

Sumimoto H, Imabayashi F, Iwata T, Kawakami Y. The BRAF-MAPK signaling pathway is essential for cancer-immune evasion in human melanoma cells. J Exp Med 2006;203:1651–6.

Taube JM, Anders RA, Young GD, Xu H, Sharma R, McMiller TL, et al. Colocalization of inflammatory response with B7-h1 expression in human melanocytic lesions supports an adaptive resistance mechanism of immune escape. Sci Transl Med 2012;4:127–37.

Thompson JF, Soong S-J, Balch CM, Gershenwald JE, Ding S, Coit DG, et al. Prognostic significance of mitotic rate in localized primary cutaneous melanoma: an analysis of patients in the multi-institutional American Joint Committee on Cancer melanoma staging database. J Clin Oncol 2011;29:2199–205.

Tumeh PC, Harview CL, Yearley JH, Shintaku IP, Taylor EJM, Robert L, et al. PD-1 blockade induces responses by inhibiting adaptive immune resistance. Nature 2014;515:568–71.

Vallacchi V, Vergani E, Camisaschi C, Deho P, Cabras AD, Sensi M, et al. Transcriptional profiling of melanoma sentinel nodes identify patients with poor outcome and reveal an association of CD30(+) T lymphocytes with progression. Cancer Res 2014;74:130–40.

Waldhauer I, Steinle A. Proteolytic release of soluble UL16-binding protein 2 from tumor cells. Cancer Res 2006;66:2520–6.